REVIEW ARTICLE

Real-time NMR measurements of protein folding and hydrogen exchange dynamics

Abani K. Bhuyan and Jayant B. Udgaonkar*
National Centre for Biological Sciences, UAS–GKVK Campus, Bangalore 560 065, India

Results of recent time-resolved NMR spectroscopy project it as one of the more powerful techniques to unravel the structural and dynamical events accompanying polypeptide folding and protein backbone amide hydrogen exchange. It has been possible to interpret the NMR-derived experimental results in the context of energy landscape model of folding and dynamics. Existing methodologies and availability of high resolution spectrometers provide opportunities to address the folding problem by way of a variety of experiments.

FOURIER techniques have revolutionized the use of NMR as a major structural tool in biology and medicine[1,2]. Multi-dimensional heteronuclear methods[3] are now used routinely to solve protein structures in native[4,5] and unfolded states[6]. The availability of resonance assignments facilitates mapping the main-chain and side-chain dynamics in the folded state[7,8], in unfolded conformations[8–10], and in protein–protein complexes[11], that would aid identification of functionally important protein motions in the picosecond to millisecond range[12]. During the past ten years NMR has also found considerable applications in studies of protein folding and hydrogen exchange (HX) reactions. The applications, for example structural description of protein folding intermediates[13–15] and partially unfolded equilibrium forms[16–18], and derivation of folding rates within a limited range of denaturant concentration[19], have employed equilibrium NMR methods that can provide kinetic information. These methodologies and results of applications have been reviewed at length[20–22]. Measurements of protein folding and HX rates in real time, another major advantage rendered by the Fourier technique and aided by the sensitivity of high resolution NMR spectrometers, have been scarce until very recently. Real-time NMR can provide, in principle, residue-level information on the kinetic excursion of a random polypeptide towards the native state.

Given that a large majority of polypeptides fold in a few milliseconds to seconds, most of the present knowledge of protein folding kinetics has been derived from traditional stopped-flow studies employing optical absorbance, fluorescence, and circular dichroism (CD) as monitoring probes. Details of structural events at atomic level can be extracted if the protein at various stages of folding is interrogated by the use of NMR, but the long time required for NMR observation compounded by several technical difficulties including the strict requirement of high sensitivity spectrometers, have limited the routine use of NMR in protein folding studies. Progress has, however, been made in recent years, and NMR is emerging as the major technique for real-time observation of structure and dynamics of polypeptides in the course of folding. Some experimental techniques useful for protein folding studies have been reviewed recently[23]. In this article, recent studies of protein folding and hydrogen exchange dynamics using high resolution NMR spectroscopy have been reviewed. The discussion summarizes some important results obtained from NMR, and compares these with optically-probed kinetic studies.

Real-time NMR vs dynamic NMR

Dynamic NMR utilizes the effect on the NMR line shape of chemical exchange across conformational equilibria. For example, in a two-state $F \leftrightarrow U$ equilibrium, where F and U are populations of folded and unfolded molecules of the protein, there is no net exchange of equilibrium magnetization. The exchange of a nucleus between the two environments of F and U during spectral acquisition affects, however, the line shape and chemical shift of the nucleus relative to the values in the absence of exchange. Simulation of line shapes using the equations for amplitude as a function of frequency[24,25] yields the first order rates for folding and unfolding, k_f and k_u. This approach has been exploited to extract submillisecond rates of folding of monomeric λ repressor in the transition region where the $F \leftrightarrow U$ equilibrium is well defined[19]. It is clear that under moderate to strongly folding or unfolding conditions where the equilibrium constant assumes values too large or too small, line shape analyses cannot be carried out.

In contrast, real-time NMR involves creation of a non-equilibrium situation ($F \rightarrow U$ or $U \rightarrow F$) by rapid initiation of the reaction followed by transient acquisition of a series of spectra as the reaction proceeds to equilibrium. In this situation the backward rate can often be neglected. Implicit in the two-state non-equilibrium condition is that

*For correspondence. (e-mail: jayant@ncbs.res.in)

the line width of product resonances will not be affected. Under favourable conditions, the time-decays of resonance integrals of identified peaks yield the resonance-specific reaction rates and amplitudes in a straightforward manner. Depending on the nature of the problem, real-time NMR can be technically and analytically challenging.

Initiation of reactions for NMR measurement of fast kinetics

All approaches used for rapid initiation of reaction for optical measurements can be adopted for NMR measurements.

Stopped-flow mixing

Design of NMR stopped-flow cells having dead-times of 2–15 ms for applications in chemistry and biochemistry were described several years ago[26,27]. Recently, a cell of 100 ms dead-time has been adopted for real-time NMR studies of *E. coli* dihydrofolate reductase (DHFR) folding[28]. When reaction time constants are greater than 2 s, for example in proline isomerization-coupled folding or HX under retarding conditions, solutions contained in two or more gas-tight syringes can be injected directly by the use of narrow Teflon flow lines into the NMR tube placed inside the magnet. The procedure involves only a little extra hardware, and the flow turbulence is sufficiently good to produce complete mixing in 2–10 s. Figures 1 and 2 show two series of representative spectra depicting the slow phase(s) of folding and unfolding of barstar, a bacterial ribonuclease inhibitor, acquired by this procedure.

Photochemical triggers

An elegant approach to examine the surface exposure of aromatic side chains is photo-Chemically Induced Dynamic Nuclear Polarization (CIDNP)[29], in which polarization of side-chain proton nuclei of histidine and aromatic residues, induced by a photoexcited dye molecule, is studied by monitoring the resultant strong and transient absorption and/or emission signals in the NMR spectra. The induction of nuclear spin polarization provides a measure of accessibility of the dye to these sites. A CIDNP experiment can be performed at equilibrium and does not require rapid solution mixing in general. But transient initiation of folding will be necessary for mapping the burial of polarizable groups as a function of folding time. Following initiation of folding, the polarization of the ring protons is examined at different times by exciting a dye using a light flash of a few tens of milliseconds of duration[30].

In certain special cases, laser photolysis can cause chain collapse and folding. The prototype of this class of experiments was described for horse ferrocytochrome *c* in which photolysis of a carbon monoxide molecule bound to the heme iron under mildly denaturing conditions drives the denatured polypeptide into a compact form[31]. In another version of this experiment, refolding of ferrocytochrome *c* was initiated within a narrow range of denaturant concentration by using an optical trigger method that rapidly injects an electron into the ferric heme of unfolded ferricytochrome *c* (ref. 32). Since both processes, photolysis of carbon monoxide and electron

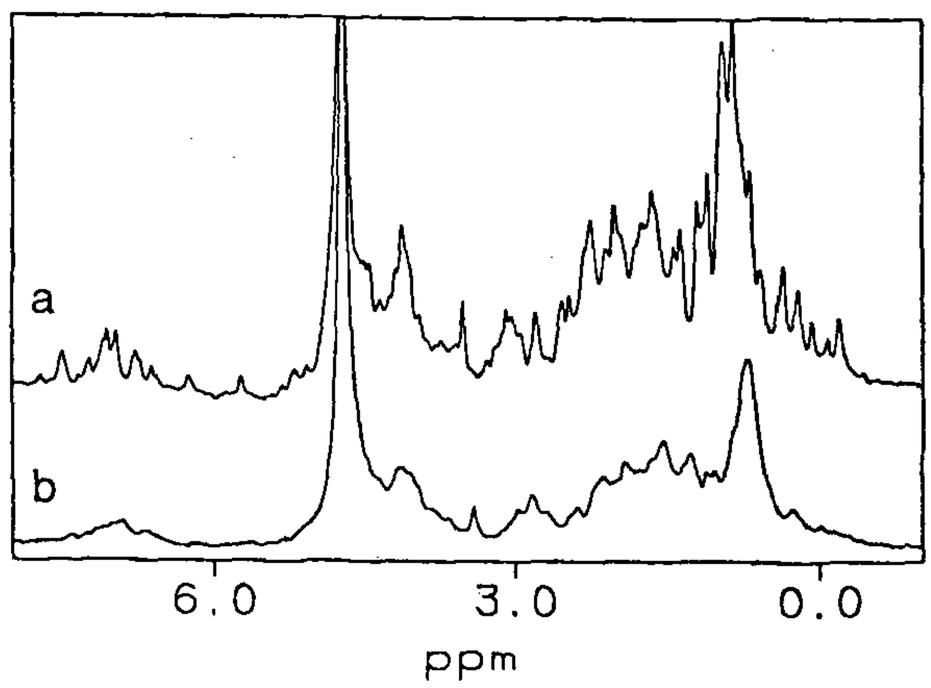

Figure 1. Some aliphatic resonances in an array of 600 MHz spectra recorded during folding (0.6 M GdnDCl) of barstar at 24°C. The unfolded protein (prepared in 20 mM phosphate buffer, ~ 300 µM EDTA, ~ 250 µM DTT, and 6 M GdnDCl, pH 8.0) and the refolding buffer (20 mM phosphate buffer, ~ 300 µM EDTA, ~ 250 µM DTT, pH 8.0), both contained in gas-tight glass syringes were injected simultaneously in 1:9 ratio into the NMR tube through narrow Teflon or plastic flow lines. The final protein concentration was ~ 1 mM. Following injection of solutions, 512 FIDS were collected in arrayed mode. The dead time of measurement determined in a separate control experiment was 7 s. Only the first 128 spectra are shown, and only those resonances are labelled which can be identified unambiguously in a one-dimensional spectrum. Shown boxed are slices at $t = 7$ s, i.e., the 'zero' time of NMR measurement (b), and at $t = 22$ min (a).

transfer, occur in far less than a microsecond[33,34], refolding can be initiated with virtually no time limitation. Neither method has thus far been exploited in NMR studies of protein folding kinetics.

Perturbation of physical variables

Generation of transient non-equilibrium states by temperature and pressure perturbation (*T*-jump and *P*-jump, respectively) of chemical equilibria is widely used in studies of enzymatic and ligand-binding reactions, and in protein folding studies. From recent developments in fast *T*-jump methodology[35], for example laser-induced temperature jumps via internal conversion of an energy transducer dye or via OH overtone relaxation in water, it is now possible to obtain temperature differentials of 30 K in nanosecond time scale[36,37]. *T*-jump can thus be used for direct observation of fast folding processes, including chain contraction and collapse, and the earliest structural reorganizations within the condensed form[37–39]. These methods are, however, not readily available for application in NMR, mainly because of the strict requirement of heating a large volume of NMR sample. *T*-jumps by heat conduction from a thermal bath[40,41], or from a gas flow[42,43] are very slow, and can provide jumps only by 10–20 K. Recently, a microwave *T*-jump NMR system that produces a jump of ~ 25 K in less than 20 ms and is suitable for aqueous solutions has been developed[44]. Improvement in efficiency of energy conversion, and the use of higher microwave power source will facilitate achieving jumps of larger magnitude in shorter time.

Equilibrium studies of the pressure effect on the structure, folding and ligand binding properties of proteins by the use of optical methods[45,46] and by NMR[47–52] have been reported, but only two studies of fast pressure jump have been published. A few years ago, a repetitive pressure perturbation technique, in which the relaxation of the reaction system to a new equilibrium is monitored after subjecting it to a small pressure jump (~ 15 bar), was used in heme absorbance-monitored millisecond kinetic studies of folding of horse ferricytochrome *c* (ref. 53). Very recently, a microsecond pressure jump method, in which the pressure could be changed by 160 bar within less than 100 μs, has been described[54]. The technique has been used for microsecond folding studies of cold shock protein[54]. Similar approaches can be adopted for NMR studies using a suitably designed NMR cell.

Some important results, interpretations, and comparison with optical data on protein folding

Chain condensation and collapse

Folding and unfolding of only a small set of proteins have been examined by kinetic NMR methods, and millisecond or faster events have rarely been monitored. In this respect, real-time optical measurements, which have begun to give information about ultrafast signals of protein folding, have a leading edge. When an unfolded polypeptide is transferred rapidly to a folding milieu, the chain responds by self-contraction and almost instantaneous collapse. The details of collapse kinetics are not understood well, but they give rise to submillisecond changes in the observable spectroscopic signal[31,32,37,38,55–58]. The structural nature of condensed products has been elusive. They have been implicated in guiding the chain specifically to the native state[58,59]. It is also held that the ultrafast signals are due to a general response of the unfolded chain when driven to folding conditions[55,60]. Snapshots of CIDNP spectra of hen lysozyme recorded at different refolding times have suggested that the rapidly formed collapsed state is disordered, and that structural reorganizations within this state are complete within a second to form apparently the native state[23,30]. For a detailed examination of kinetic events and structural nature of the collapsed chain at individual amino acid residue level, development of NMR methods for faster kinetics will be essential.

Detection of structural intermediates during protein unfolding

While the formation and the accumulation of intermediates during folding have been recognized for a long time to be common events in the folding of many proteins, it was not believed until recently that structural intermediates may also populate during protein unfolding, perhaps because unfolding concentrations of denaturants might destabilize largely any structure that may be retained. In a rather long dead-time (> 1 min) measurement of unfolding of ribonuclease A, where unfolding was initiated outside the magnet probe by mixing the protein solution with a solution of guanidinium deuterochloride (GdnDCl, prepared by repeated lyophilization of GdnHCl dissolved in D_2O), it was shown that the kinetics of disappearance of the intensity of a side-chain resonance resolved in the up field region of the spectrum is distinctly different from the unfolding kinetics measured by CD at both far-UV and near-UV regions[61]. This result, which indicated the accumulation of a partially retained structure, provided a landmark demonstration that intermediates can also populate during unfolding. Almost at the same time, stopped-flow ^{19}F NMR data on unfolding of *E. coli* DHFR showed rapid formation of an intermediate containing substantial secondary structure and native-like fluorescence, but possessing side chain mobility[62].

Detection of native-like contacts in folding intermediates

Defining the structural and energetic properties of protein intermediates is important to understand the nature of

protein folding pathways, and NMR is the only method that can provide the structural details, unless the intermediates are trapped and crystallized for X-ray analysis. Transient mixing protocols, in which an unfolded deuterated protein is exposed to proton pulses at different times of folding, can be used to label the backbone amide sites to examine the extent of structure formation, because a structured segment will protect the amide sites from proton labelling. In a recent real-time experiment with α-lactalbumin[63], specific native-like contacts between residues have been detected in the molten globule state by observation of Nuclear Overhauser Effects (NOEs). The molten globule state, prepared by dissolving the protein at pH 2, is a long-lived species and is taken to be a major folding intermediate. Immediately after saturating the aromatic region of the NMR spectrum of the molten globule by high power continuous radio frequencies, the molten globule is refolded to the native state by transient mixing with a buffer at pH 7, and the effect of saturation is monitored by NOE enhancement of the aliphatic resonances in the native-state spectrum. An NOE build-up curve can be obtained by plotting the resonance enhancement as a function of time of irradiation of the aromatic envelope in the molten globule state. By comparing the build-up curves for the molten globule and the native state of the protein, it was found that NOEs between residues in the molten globule state are similar in overall intensity to those in the native state[63]. An exciting prospect of this method is mapping the nature and the order of a range of contacts between residues, so folding structures can be observed in more detail.

Multi-state kinetics of protein folding and unfolding

Kinetics of formation or dissolution of tertiary and secondary structures are recorded by monitoring tryptophan fluorescence and near-UV circular dichroism (CD), and far-UV CD, respectively. In a number of classic folding studies, the kinetic parameters measured by fluorescence and near-UV CD have been found to be different from those measured by far-UV CD[64]. This and similar observations provided evidence that proteins must fold via a few discrete intermediates[59,64,65]. An intermediate, for example, may have almost fully formed secondary structure but only marginally stable tertiary structures[66,67]. More recent ideas emanating from statistical characterization of the energy landscape of folding proteins suggest that the energy surface is highly rugged, so it is not just one or a few discrete intermediates, but a large number of intermediates that populate during folding[68–72], and the presence of these intermediates leads to multi-state kinetics as a result of transient trapping of structures that are either partially folded or misfolded. Indeed, microsecond folding kinetics studied by time-resolved CD and magnetic circular dichroism (MCD) following laser photolysis of a carbon monoxide molecule liganded to the iron atom of denatured ferrocytochrome *c* (see above) show that proteins can fold via multiple pathways[73]. By virtue of its ability of interrogating a large number of residue-specific sites, real-time NMR studies have provided the strongest evidence for the multi-state nature of protein-folding kinetics. Refolding studies of 6-^{19}F-tryptophan labelled *E. coli* DHFR had indicated earlier that during the first 20 s of refolding, regions of the protein around some tryptophan residues may form native-like tertiary contacts earlier than regions around some other tryptophans, but the native-like contacts formed are either unstable and exchange between native and non-native forms, or reflect a distribution of heterogeneous side chain environments within a native-like overall structure[74]. More elaborate real-time NMR studies of folding and unfolding of barstar, revealed heterogeneous kinetics in respect to both the fraction of the expected amplitudes lost during the dead-time of measurement (10 s) and the denaturant dependence of observed rates for a sizeable set of spatially distant protons whose resonances could be unambiguously identified in the spectra (Figures 1 and 2). Of course, the heterogeneity in kinetics of folding and unfolding is also observed when the folding and unfolding reactions of barstar are monitored by fluorescence, and near- and far-UV CD. These results have provided an unprecedented observation of a large ensemble of partially folded states during folding and unfolding in agreement with the prediction of multi-state nature of protein folding kinetics[75].

Transient mixing NMR study of amide hydrogen exchange under strongly destabilizing conditions

Structural stability, polypeptide folding, functionally important conformational fluctuations, and backbone amide hydrogen exchange (HX) with the bulk solvent are closely tied in protein studies. HX has played a major role in temporal resolution of protein folding intermediates[15], structural description of non-native compact states[76], observation of allosteric changes in proteins[77], and detection of partially unfolded states that are suggested to be concatenated to form sequential folding pathways[16–18]. These studies are generally done by holding the protein solutions at equilibrium under native or native-like conditions where the amide hydrogens of many native proteins exchange over several hours to weeks, and the time dependence of exchange of the hydrogens with solvent deuterium can be observed conveniently by recording a series of 2D NMR spectra at different time intervals.

It is, however, equally important to test the HX behaviour under non-native conditions. A particularly pressing point to settle is whether the partially unfolded states detected under native-like conditions exist even

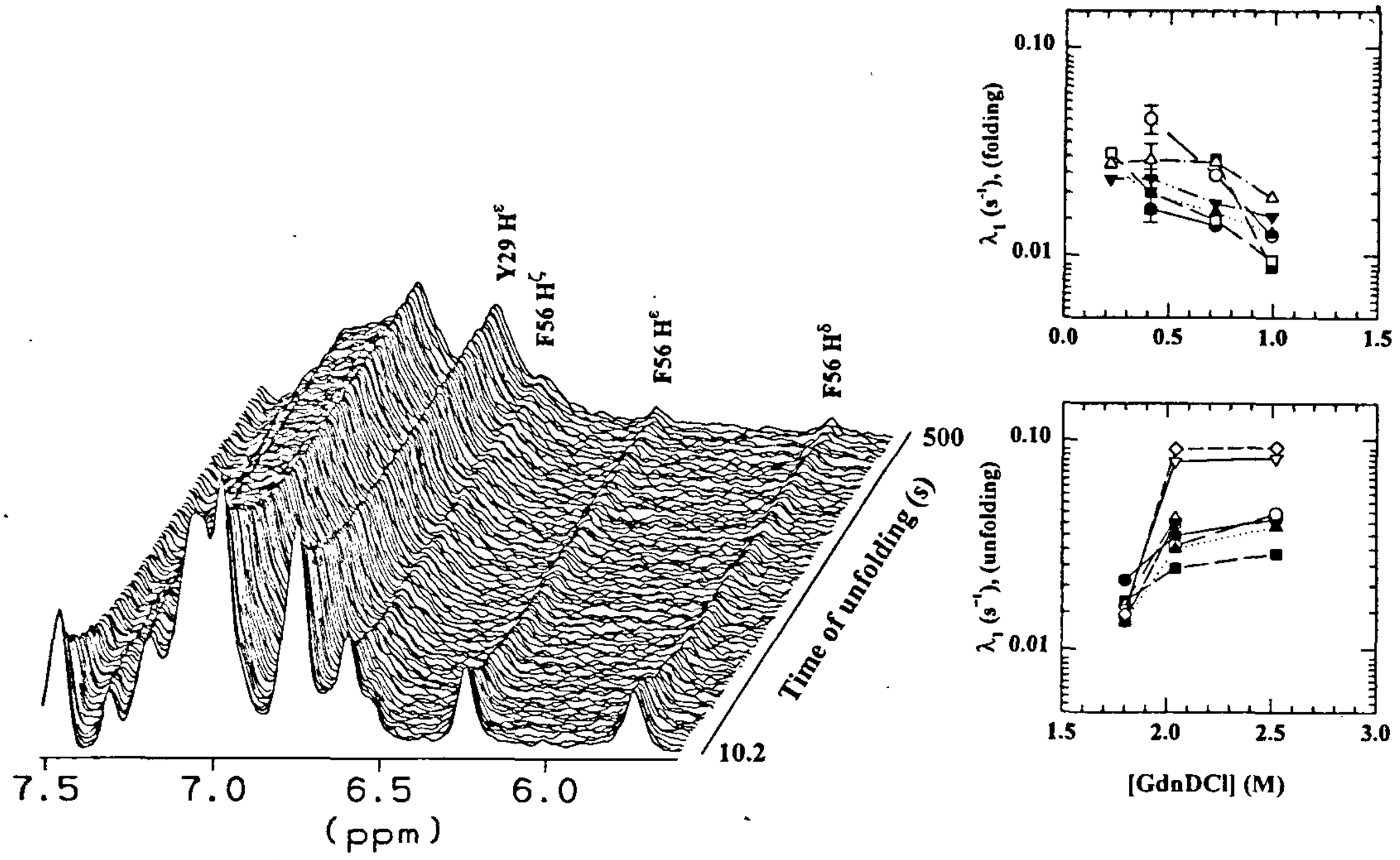

Figure 2. An expanded view of the aromatic region during unfolding (1.8 M GdnDCl) of barstar. The buffers and the experimental conditions were same as in Figure 1. In order to obtain the denaturant dependence of appparent rates of folding and unfolding, the experiments were done in the presence of different concentrations of GdnDCl. The two panels at the right show the denaturant distribution of apparent rates of folding and unfolding for a number of resonances (●, L20 Hδ2; ○, L41Hδ1; ■, L51Hδ2; □, I5Hγ2; ▲, L26Hδ1; Δ, F56Hε; ▼, F56Hδ; ∇, W53CαH; and an *unassigned resonance (◊) at 7.47 ppm of the unfolded polypeptide). The lines are drawn by inspection only. Dispersion in the rates along with* denaturant distribution of other spectral features (see text) have been interpreted as one of the indications of muti-state nature of folding and unfolding kinetics. The two panels showing the denaturant dependence of rates are taken from ref. 74.

under denaturing to unfolding conditions. When the solvent conditions are sufficiently destabilizing for the protein structure, the kinetics of HX reactions are, however, too fast, typically few tens of seconds or less, and are immeasurable unless the exchange reaction is initiated by transient mixing of solutions. The situation calls for stopped-flow initiation of the HX reaction in which the native protein dissolved in an aqueous solution is rapidly mixed with the deuterated solvent containing the protein destabilizing agent.

In the first application of real-time NMR in studies of HX, exchange kinetics of a small set of backbone hydrogens of reduced horse cytochrome *c* under strongly destabilizing conditions were recorded in two minutes (Figure 3, ref. 78). In this experiment, the protein solution and the buffer containing GdnDCl were driven into the NMR tube from two gas-tight syringes via two narrow flow lines. Since an anaerobic atmosphere was essential to keep the protein in the reduced form, a third flow line was introduced directly into the NMR tube to pass a gentle flow of argon over the solution at all stages of the experiment.

The results of such measurements provide resolution of both energetics and the mechanism of protein HX. The analyses and interpretation of HX studies under any solvent condition suffer from the uncertainty of the actual exchange mechanism: EX1 or EX2. For the general scheme[79]

$$\text{closed (H)} \underset{k_{cl}}{\overset{k_{op}}{\Leftrightarrow}} \text{open (H)} \xrightarrow{k_{cl}} \text{open (D)},$$

where k_{op} and k_{cl} are rate constants for opening and closing of an amide site, and k_{ch} is the exchange rate of the same amide site in the unstructured polypeptide, the experimentally observed exchange rate is given by $k_{ex}^{obs} = k_{op}k_{cl}/(k_{op} + k_{cl} + k_{ch})$. In the EX2 limit, expected under native-like conditions where $k_{cl} \gg k_{op}$, k_{ch}, $k_{ex}^{obs} \approx K_{op}k_{ch}$ (where $K_{op} = k_{op}/k_{cl}$ is the equilibrium constant for the HX-related fluctuational motion), and in the EX1 limit expected under strongly destabilizing conditions, where the magnitude of k_{op} approaches that of k_{cl} and k_{op}, $k_{cl} \ll k_{ch}$, $k_{ex}^{obs} \approx k_{op}$. The analytical treatment of k_{ex}^{obs} values obtained from HX kinetic traces like those shown in Figure 3 *a* can be done by assuming EX1 or EX2, but the choice of EX1 or EX2 depends on the balance of k_{cl} and k_{op}, that in turn is dependent on how stable an exchanging structure is. There is no direct way of knowing if the EX2 mechanism, which operates normally under native-like conditions (see refs 80–82),

holds also under strongly destabilizing conditions. The results of real-time NMR (Figure 3) resolves this issue. The denaturant dependence of the free energy of hydrogen exchange, ΔG_{op}, calculated in the EX2 formalism (Figure 3 *b*; see the Figure legend for calculation procedure) converges to zero at the midpoint of the unfolding transition (where $K_{op} = k_{op}/k_{cl} = 1$), suggesting the validity of EX2 analysis. Furthermore, the isoenergetic behaviour of the HX reactions illustrated for the four protons suggests the existence of at least one partially unfolded structure formed of the resident segments of these protons[78]. These studies will be potentially useful to understand the complexity of the coupling between protein motions and stabilization of protein folding intermediates.

Experimental difficulties

The need for a large volume of highly concentrated protein solutions, and the requirement of mixing solutions within the NMR probe are the two major practical problems in real-time experiments. Large volumes of protein and buffer solutions are needed because of the use

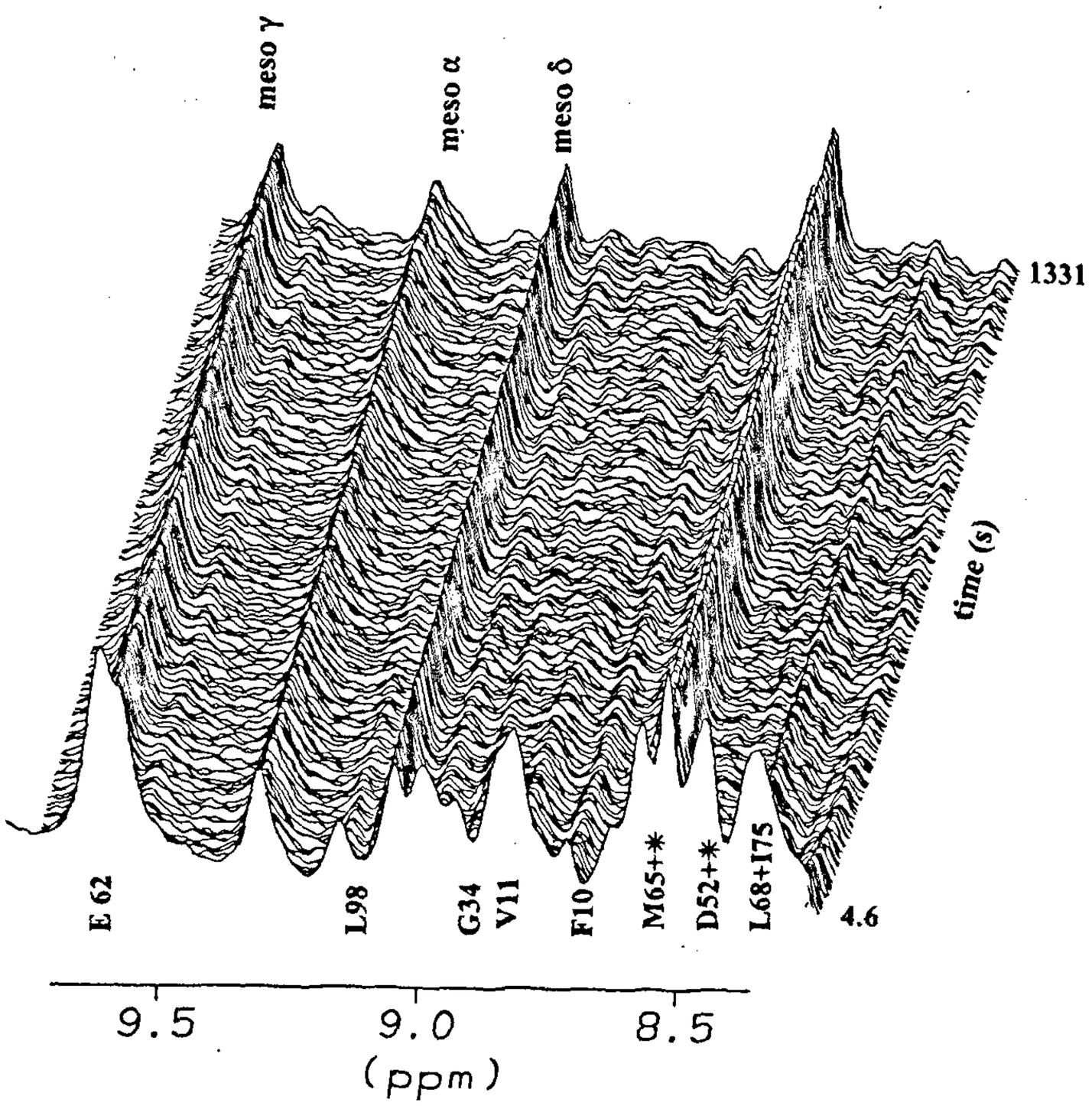

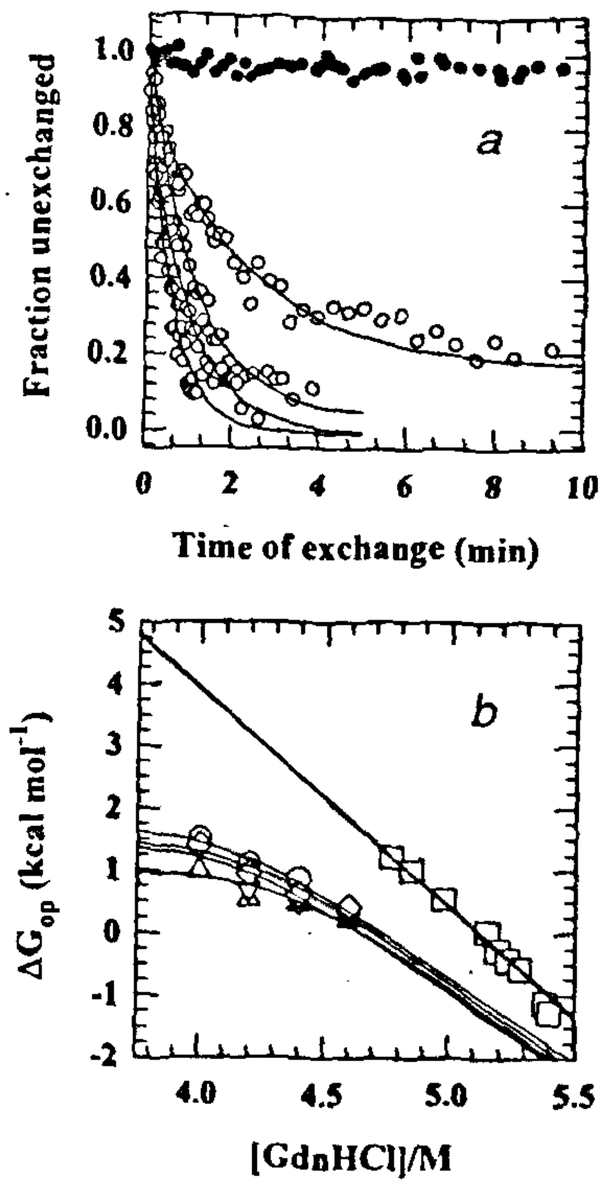

Figure 3. Stack plot display of 600 MHz NMR spectra of reduced cyt *c* following initiation of hydrogen exchange in 4 M GdnDCl at 24°C. Spectra up to the 256th FID are shown with a row increment of 2. Chemical shifts and intensities of other resonances in the spectra remain constant throughout the course of the experiment. The meso protons of the heme porphyrin ring also do not appear to exchange in the range of GdnDCl used. After 1 : 9 mixing of the dithionite-reduced aqueous protein solution and the deuterated buffer, both prepared in 0.1 M phosphate buffer and the latter containing GdnDCl, the final medium for HX contained 1.2–1.5 mM cytochrome *c*, 90% D_2O, 23 mM sodium dithionite, and 4 M GdnDCl at pH 6. The reported pH value is the corrected glass electrode reading recorded after HX measurements. Spectra were recorded in a Varian Unity plus spectrometer operating at a ^1H frequency of 600.051 MHz. The spectral width was 10101 Hz. Each series of spectra was arrayed to 512 FIDs with no preacquisition delay in between. An FID was an average of 2 or 4 scans. Water suppression was achieved by on-resonance irradiation of the signal during the relaxation delay of 1 s. All experiments were done at 24°C. Data were processed using Felix 95 (BIOSYM) and VNMR software provided by Varian Associates. The inaccuracy in intensity measurement was approximately ± 7%. *a*, The GdnDCl-dependence of the observed kinetics for the NH exchange of V11. The rate increases in the order: 4, 4.2, 4.4, and 4.6 M GdnDCl. This panel also shows the constant intensity of the M80εCH$_3$ resonance (●) plotted on a single proton basis which indicates that the protein stayed reduced and that the spectral changes are due only to HX. *b*, GdnDCl dependence of ΔG_{op} ($= -RT \ln[K_1 + K_u^0 e^{m[GdnDCl]/RT}(1 + K_1)]$, where K_1 and K_u^0 are equilibrium constants for local structure opening in the presence of a given concentration of GdnDCl and the global unfolding event in the absence of denaturant, respectively) for L98 (○), V11 (△), F10 (▽), and Y97 (◇). These residues form the amino and the carboxyl terminal helix of cytochrome *c*. On the basis of strikingly similar exchange energies (ΔG_{op}) and denaturant gradient of ΔG_{op} values for these residues, the two terminal helices appear to define a subglobal structural unit displaying a common cooperative structure opening reaction. The solid straight line through the far-UV CD monitored equilibrium unfolding data (□) describes the denaturant dependence of global free-energy of folding. The exchange mechanism is EX2 because the bunch of ΔG_{op} curves, defining the free-energy of the subglobal structural unit, approach zero instead of converging to unity in the global unfolding transition region. The EX2 condition is validated also by the observation that the ΔG_{op} curves for these protons at the unfolding transition region do not take an upward turn towards positive values. The data have been taken from ref. 78 with permission.

of long flow lines and the requirement of ~ 500 µl of mixed solutions to fill the space inside the coil. The protein concentration problem can be overwhelming when a large dilution is required to refold (or unfold) the protein. The situation worsens when measurement of time constants of 10 s or less is attempted, because each spectrum now may have to be generated from a single FID so the protein concentration in the final folding medium must be held high. Worse yet is the requirement that the spectra be collected in a relatively less homogeneous field, and often in the presence of high concentration of denaturants.

A sufficient volume (~ 500 µl) of thoroughly mixed solution is essential for better NMR sensitivity. In this regard performing optical experiments is more convenient, where a sample volume as little as the size of a tightly focused beam is sufficient. This also facilitates sufficient signal averaging within a short time.

Two-dimensional (and multi-dimensional) real-time NMR

Transient mixing real-time measurements ($\tau > 10$ s) are done by generating arrayed 1D spectra, and hence, only a small set of resonances can be identified confidently. For slower reactions that go to completion in ~ 15–20 min or more, a series of fast 2D spectra, each consuming about 2–3 min, can be recorded by replacing phase cycles with field gradients inserted appropriately into pulse sequences. Folding studies of collagen triple-helix provide an example of fast 2D spectral recording[83]. The folding transition from denatured monomer peptides to a supercoiled helical trimer is sufficiently slow, so a series of 2D ^{1}H–^{15}N HSQC spectra of ^{15}N-labelled peptides could be recorded during refolding. 2D 15-N edited spectra have also been recorded in a very recently concluded study to follow the *trans–cis* interconversion of the Y47–P48 bond during the folding of barstar[84].

For a slow one-sided reaction of the type $F \rightarrow U$ (or $U \rightarrow F$), a single 2D spectrum collected during the course of folding can substitute for an array of spectra in terms of information content. If the folding reaction continues to progress during systematic pulse delay incrementations (t_1), the equilibrium magnetization of a nucleus in F or U is different for different t_1, and therefore, the signals in the 2D spectrum will also be a function of the folding rate, k_f. The intensities and line-shapes of a resonance from F and U in the indirect t_1 dimension can then be simulated and minimized to obtain the first order rate constant[27,85,86]. A complete line shape analysis of resolved resonances in t_1 slices is laborious and time consuming. Nevertheless, the approach does give meaningful information about the folding kinetics for a large set of resonances. Finally, one may look for the possibility of obtaining triple resonance 3D spectra of different versions if the folding and unfolding reactions are very slow, or made slower if not slow inherently. Heteronuclear multidimensional spectra can be recorded in a few hours by the use of pulsed field gradients[87].

Improvement in time resolution

The dead-time of 100 ms reported in the work with dihydrofolate reductase[28,62] can be shortened without considerable technical difficulty. However, faster mixing and shorter dead-time may not provide significant advantage in studies of slow folding and unfolding reactions. Faster folding rates (hundreds of milliseconds of τ) have not been measured by NMR. Shorter dead-time will aid such measurements. For reactions still faster (hundreds of microseconds of τ) that occur during the collection of a single FID, optical and photochemical triggers[31,32], and microsecond jet mixers[88] may be introduced, but data acquisition, appropriate analyses, and interpretation will need further development of theory and methods.

Outlook

The methods and results outlined here clearly indicate the potential of time-resolved NMR in studies of protein folding and dynamics. Experiments with objectives of identification of the extent and the range of NOEs in collapsed polypeptides and in partially folded protein states generated by double jump protocols, detection of resonance shifts and line-broadening in transient species, and determination of relaxation dynamics (T_1, T_2, NOE, aromatic ring flip rates, and side chain motions) in relatively long-lived intermediates will be indispensable in the endeavour of solving the protein folding problem. With regard to HX, measurement of NOE between adjacent labile protons will resolve whether exchange occurs in the EX1 limit or in the EX2 in a given experimental situation[20]. During the past decade, NMR methods for protein studies have advanced significantly and rapidly, so exciting applications to the folding problem lie ahead.

1. Ernst, R. R., Bodenhausen, G. and Wokaun, A., *Principles of Nuclear Magnetic Resonance in One and Two Dimensions*, Clarendon Press, Oxford, 1987.
2. Wüthrich, K., *NMR of Proteins and Nucleic Acids*, John Wiley, 1986.
3. Oschkinat, H., Muller, T. and Dieckmann, T., *Angew. Chem. Int. Ed. Engl.*, 1994, **33**, 277–293.
4. Clore, G. M. and Gronenborn, A. M. (eds), in *NMR of Proteins*, Macmillan, 1993, pp. 1–27.
5. Kay, L. E. and Gardner, K. H., *Curr. Opin. Struct. Biol.*, 1997, **7**, 722–731.
6. Neri, D., Billeter, M., Wider, G. and Wüthrich, K., *Science*, 1992, **257**, 1559–1563.
7. Kay, L. E., Muhandiram, D. R., Farrow, N. A., Aubin, Y. and Forman-Kay, J. D., *Biochemistry*, 1996, **35**, 361–368.

8. Farrow, N. A., Zhang, O., Forman-Kay, J. D. and Kay, L., *Biochemistry*, 1995, **34**, 868–878.
9. Penkett, C. J., Redfield, C., Jones, J. A., Dodd, I., Hubbard, J., Smith, R. A. G., Smith, L. J. and Dobson, C. M., *Biochemistry*, 1998, **37**, 17054–17067.
10. Meekhof, A. E. and Freund, S. M. V., *J. Mol. Biol.*, 1999, **286**, 579–592.
11. Sahu, S. C., Bhuyan, A. K., Udgaonkar, J. B. and Hosur, R. V (submitted).
12. Palmer, A. G., III, *Curr. Opin. Struct. Biol.*, 1997, **7**, 732–737.
13. Udgaonkar, J. B. and Baldwin, R. L., *Nature*, 1988, **335**, 694–699.
14. Roder, H., Elöve, G. A. and Englander, S. W., *Nature*, 1988, **335**, 700–704.
15. Englander, S. W. and Mayne, L., *Annu. Rev. Biophys. Biomol. Struct.*, 1992, **21**, 243–265.
16. Bai, Y., Sosnick, T. R., Mayne, L. and Englander, S. W., *Science*, 1995, **269**, 192–196.
17. Chamberlain, A. K., Handel, T. M. and Marqusee, S., *Nat. Struct. Biol.*, 1996, **3**, 782–787.
18. Bhuyan, A. K. and Udgaonkar, J. B., *Proteins: Struct. Funct. Genet.*, 1998, **30**, 295–308.
19. Huang, G. S. and Oas, T. G., *Proc. Natl. Acad. Sci. USA*, 1995, **92**, 6878–6882.
20. Wagner, G. and Wüthrich, K., *Methods Enzymol.*, 1986, **131**, 307–326.
21. Roder, H., *Methods Enzymol.*, 1989, **176**, 446–472.
22. Dyson, H. J. and Wright, P. E., *Annu. Rev. Phys. Chem.*, 1996, **47**, 369–395.
23. Dobson, C. M. and Hore, P. J., *Nat. Struct. Biol.*, 1998, **5**, 504–507.
24. Sandström, J., *Dynamic NMR Spectroscopy*, Academic Press, 1982.
25. McConnell, H. M., *J. Chem. Phys.*, 1958, **28**, 430–431.
26. Grimaldi, J. J. and Sykes, B. D., *Rev. Sci. Instrum.*, 1975, **46**, 1201–1205.
27. Kühne, R. O., Schaffhauser, T., Wokaun, A. and Ernst, R. R., *J. Magn. Reson.*, 1979, **35**, 39–67.
28. Hoeltzli, S. D., Ropson, I. J. and Frieden, C., *Tech. Protein Chem.*, 1994, **V**, 455–466.
29. Hore, P. J., Egmond, M. R., Edzes, H. T. and Kaptein, R., *J. Magn. Reson.*, 1982, **49**, 122–150.
30. Hore, P. J., Winder, S. L., Roberts, C. H. and Dobson, C. M., *J. Am. Chem. Soc.*, 1997, **119**, 5049–5050.
31. Jones, C. M., Henry, E. R., Hu, Y., Chan, C. K., Luck, S. D., Bhuyan, A., Roder, H., Hofrichter, J. and Eaton, W. A., *Proc. Natl. Acad. Sci. USA*, 1993, **90**, 11860–11864.
32. Pascher, T., Chesick, J. P., Winkler, J. R. and Gray, H. B., *Science*, 1996, **271**, 1558–1560.
33. Anfinrud, P. A., Han, C. and Hochstrasser, R. M., *Proc. Natl. Acad. Sci. USA*, 1989, **86**, 8387–8391.
34. Northrup, S. H., in *Protein Electron Transfer* (ed. Bendall, D. S.), BIOS Scientific Publishers Limited, Oxford, 1996.
35. Chen, S., Lee, I.-Y. S., Tolbert, W. A., Wen, X. and Dlott, D. D., *J. Phys. Chem.*, 1992, **96**, 7178–7186.
36. Phillips, C. M., Mizutani, Y. and Hochstrasser, R. M., *Proc. Natl. Acad. Sci. USA*, 1995, **92**, 7292–7296.
37. Ballew, R. M., Sabelko, J. and Gruebele, M., *Proc. Natl. Acad. Sci. USA*, 1996, **93**, 5759–5764.
38. Ballew, R. M., Sabelko, J. and Gruebele, M., *Nat. Struct. Biol.*, 1996, **3**, 923–926.
39. Williams, S., Cosgrove, T. P., Gilmanshin, R., Fang, K. S., Callendar, R. H., Woodruff, W. H. and Dyer, R. B., *Biochemistry*, 1996, **36**, 691–698.
40. Blum, A. D., Smallcombe, S. H. and Baldwin, R. L., *J. Mol. Biol.*, 1978, **118**, 305.
41. Adler, M. and Scheraga, H. A., *Biochemistry*, 1988, **27**, 2471–2480.
42. Akasaka, K., Naito, A. and Nakatani, H., *J. Biomol. NMR*, 1991, **1**, 65–70.
43. Akasaka, K. and Naito, A., *Rev. Sci. Instrum.*, 1991, **61**, 66.
44. Kawakami, M. and Akasaka, K., *Rev. Sci. Instrum.*, 1998, **69**, 3365–3369.
45. Frauenfelder, H., Alberding, N. A., Ansari, A., Braunstein, D., Cowen, B. R., Hong, M. K., Iben, I. E. T., Johnson, J. B., Luck, S., Marden, M. C., Mourant, J. R., Ormos, P., Reinisch, L., Scholl, R., Schulte, A., Shyamsunder, E., Sorensen, L. B., Steinbach, P. J., Xie, A., Young, R. D. and Yue, K. T., *J. Phys. Chem.*, 1990, **94**, 1024–1037.
46. Marden, M. C., Hoa, G. H. B. and Stetzkowski-Marden, F., *Biophys. J.*, 1986, **49**, 619–627.
47. Inoue, K., Yamada, H., Imoto, T. and Akasaka, K., *J. Biomol. NMR*, 1998, **12**, 535–541.
48. Hua, L., Yamada, H. and Akasaka, K., *Biochemistry*, 1998, **37**, 1167–1173.
49. Samarasinghe, S., Campbell, D. M., Jonas, A. and Jonas, J., *Biochemistry*, 1991, **31**, 7773–7778.
50. Royer, C. A., Hinck, A. P., Loh, S. N., Prehoda, K. E., Peng, X., Jonas, J. and Markley, J. L., *Biochemistry*, 1993, **32**, 5222–5232.
51. Morishima, I., *Current Perspectives of High Pressure Biology*, Academic Press, 1987, pp. 315–333.
52. Markley, J. L., Northrop, D. B. and Royer, C. A. (eds), *High Pressure Effects in Molecular Biophysics and Enzymology*, Oxford University Press, 1996.
53. Pryse, K. M., Bruckman, T. G., Maxfield, B. W. and Elson, E. L., *Biochemistry*, 1992, **31**, 5127–5136.
54. Jacob, M., Holtermann, G., Perl, D., Reinstein, J., Schindler, T., Geeves, M. A. and Schmid, F. X., *Biochemistry*, 1999, **38**, 2882–2891.
55. Sosnick, T. R., Shtilerman, M. D., Mayne, L. and Englander, S. W., *Proc. Natl. Acad. Sci. USA*, 1997, **94**, 8545–8550.
56. Chan, C.-K., Hu, Y., Takahashi, S., Rousseau, D. L., Eaton, W. A. and Hofrichter, J., *Proc. Natl. Acad. Sci. USA*, 1997, **94**, 1779–1784.
57. Takahashi, S., Yeh, S.-R., Das, T. K., Chan, C.-K., Gottfried, D. S. and Rousseau, D. L., *Nat. Struct. Biol.*, 1997, **4**, 44–50.
58. Shastry, M. C. R. and Roder, H., *Nat. Struct. Biol.*, 1998, **5**, 385–392.
59. Roder, H. and Colón, W., *Curr. Opin. Struct. Biol.*, 1997, **7**, 15–28.
60. Qi, P. Q., Sosnick, T. R. and Englander, S. W., *Nat. Struct. Biol.*, 1998, **5**, 882–884.
61. Kiefhaber, T., Labhardt, A. M. and Baldwin, R. L., *Nature*, 1995, **375**, 513–515.
62. Hoeltzli, S. D. and Frieden, C., *Proc. Natl. Acad. Sci. USA*, 1995, **92**, 9318–9322.
63. Balbach, J., Forge, V., Lau, W. S., Jones, J. A., van Nuland, N. A. J. and Dobson, C. M., *Proc. Natl. Acad. Sci. USA*, 1997, **94**, 7182–7185.
64. Matthews, C. R., *Annu. Rev. Biochem.*, 1993, **62**, 653–683.
65. Baldwin, R. L., *J. Biomol. NMR*, 1995, **5**, 103–109.
66. Kuwajima, K., Yamaya, H., Miwa, H., Sugai, S. and Nakamura, T., *FEBS Lett.*, 1987, **221**, 115–118.
67. Ptitsyn, O. B., *Adv. Protein. Chem.*, 1995, **47**, 83–229.
68. Bryngelson, J. D., Onuchic, J. N., Socci, N. D. and Wolynes, P. G., *Proteins: Struct. Funct. Genet*, 1995, **21**, 167–195.
69. Dill, K. A. and Chan, H. S., *Nat. Struct. Biol.*, 1997, **4**, 10–19.
70. Chan, H. S. and Dill, K. A., *Proteins: Struct. Funct. Genet.*, 1998, **30**, 2–33.
71. Leopold, P. E., Montal, M. and Onuchic, J. N., *Proc. Natl. Acad. Sci. USA*, 1992, **89**, 8721–8725.
72. Onuchic, J. N., Luthey-Schulten, Z. and Wolynes, P. G., *Annu. Rev. Phys. Chem.*, 1997, **48**, 545–600.
73. Goldbeck, R. A., Thomas, Y. G., Chen, E., Esquerra, R. M. and Kliger, D. S., *Proc. Natl. Acad. Sci. USA*, 1999, **96**, 2782–2787.

74. Hoeltzli, S. D. and Frieden, C., *Biochemistry*, 1996, **35**, 16834–16851.
75. Bhuyan, A. K. and Udgaonkar, J. B., *Biochemistry*, 1999, **38**, 9158–9168.
76. Baum, J., Dobson, C., Evans, P. and Hanley, C., *Biochemistry*, 1989, **28**, 7–13.
77. Englander, S. W., Englander, J. J., McKinnie, R., Ackers, G. K., Turner, G. J., Westrick, J. A. and Gill, S. J., *Science*, 1992, **256**, 1684–1687.
78. Bhuyan, A. K. and Udgaonkar, J. B., *Proteins: Struct. Funct. Genet.*, 1998, **32**, 241–247.
79. Hvidt, A., *C. r. Trav. Lab. Carlsberg*, 1964, **34**, 299–317.
80. Loh, S. N., Rohl, C. A., Kiefhaber, T. and Baldwin, R. L., *Proc. Natl. Acad. Sci. USA*, 1996, **93**, 1982–1987.
81. Clark, J. and Fersht, A. R., *Folding Design*, 1996, **1**, 243–254.
82. Pedersen, T. G., Thomsen, N. K., Andersen, N. K., Madsen, J. C. and Poulsen, F. M., *J. Mol. Biol.*, 1993, **230**, 651–660.
83. Baum, J. and Brodsky, B., *Folding Design*, 1997, **2**, R53–R60.
84. Killick, T. R., Freund, S. M. V. and Fersht, A. R., *Protein Sci.*, 1999, **8**, 1286–1291.
85. Balbach, J., Forge, V., Lau, W. S., van Nuland, N. A. J., Brew, K. and Dobson, C. M., *Science*, 1996, **274**, 1161–1163.
86. Balbach, J., Steegborn, C., Schindler, T. and Schmid, F. X., *J. Mol. Biol.*, 1998, **285**, 829–842.
87. Bax, A. and Pochapsky, S., *J. Magn. Reson.*, 1992, **99**, 638–643.
88. Regenfuss, P., Clegg, R. M., Fulwyler, M. J., Barrantes, F. J. and Jovin, T. M., *Rev. Sci. Instrum.*, 1985, **56**, 283–290.

ACKNOWLEDGEMENTS. The support and services provided by the National Facility for High Resolution NMR, TIFR, Mumbai are most gratefully acknowledged. This research is funded by the Tata Institute of Fundamental Research and the Department of Biotechnology. J.B.U. is the recipient of a Swarnajayanti Fellowship from the Government of India.

Received 5 June 1999; revised accepted 12 August 1999.